Electronic Supplementary Material (ESI) for Physical Chemistry Chemical Physics.

Supplementary Information

An in Silico Investigation of Binding Modes and Pathway of APTO-253 on c-KIT G-Quadruplex DNA

Saikat Pal and Sandip Paul*

Department of Chemistry, Indian Institute of Technology, Guwahati Assam, India-781039

(Dated: November 30, 2020)

Disease Type	Cell Lines	$IC_{50}(\mu M)$ Mean
MCL	**Jeko-1**	0.057
MCL	**GRANTA-519**	0.082
Burkitt's	**Raji**	0.1
AML	**MOLM-13**	0.14
MCL	**Mino**	0.23
AML	**MV4-11**	0.24
AML	**EOL-1**	0.3
AML	**THP1**	0.34
Burkitt's	**Ramos**	0.35
AML	**HL-60**	0.46
AML	**SKM-1**	0.48
AML	**KG-1**	0.51
DLBCL	**SUDHL-6**	0.51
T-ALL	**Jurkat**	0.52
AML	**Nomo-1**	1.45
AML	**HEL92.1.7**	1.75

TABLE S1: APTO-253 IC_{50} values in leukemia and lymphoma cell lines.

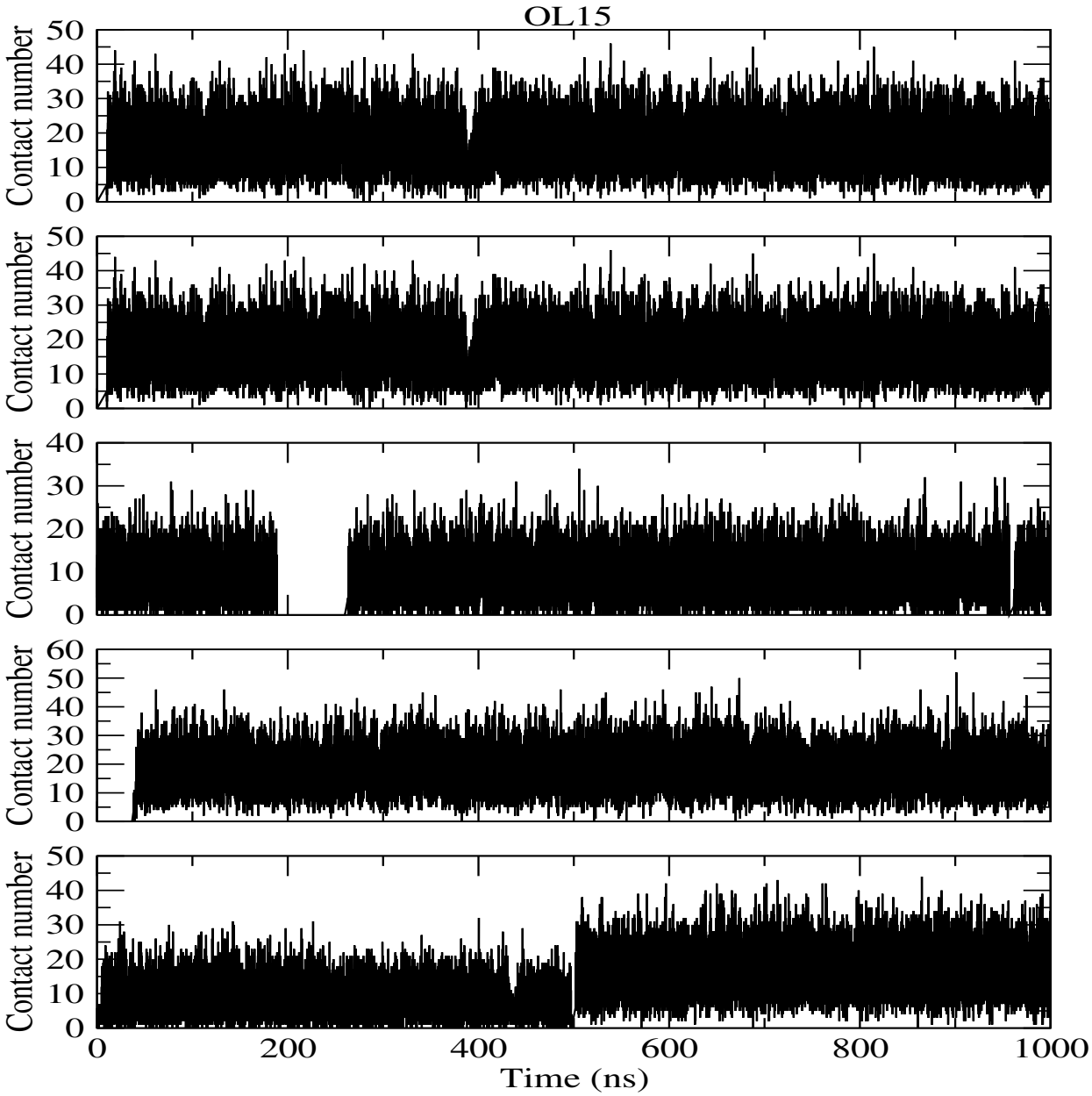

FIG. S1: Contact number between APTO-253 and c-KIT quadruplex DNA for different systems.

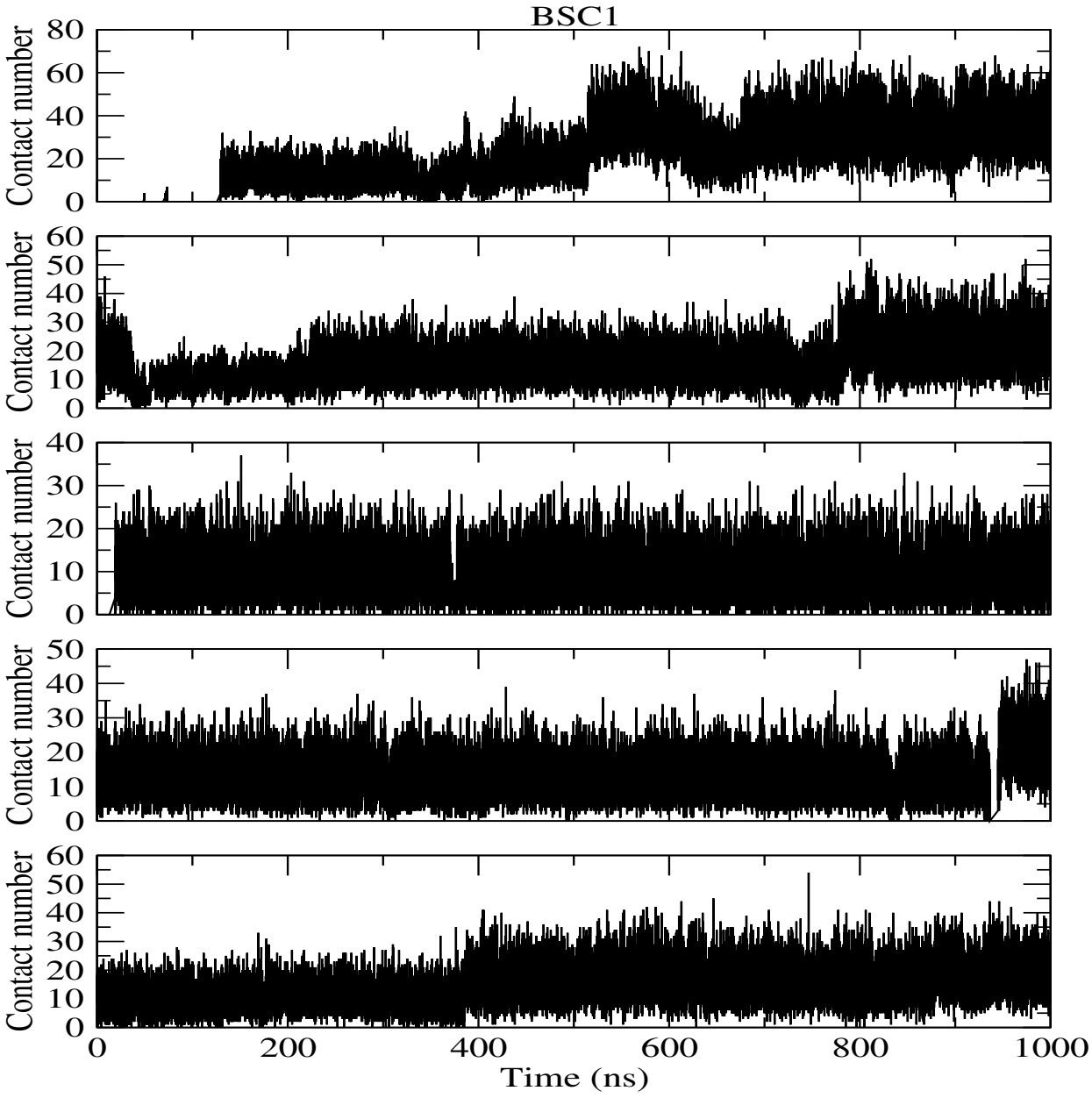

FIG. S2: Contact number between APTO-253 and c-KIT quadruplex DNA for different systems.

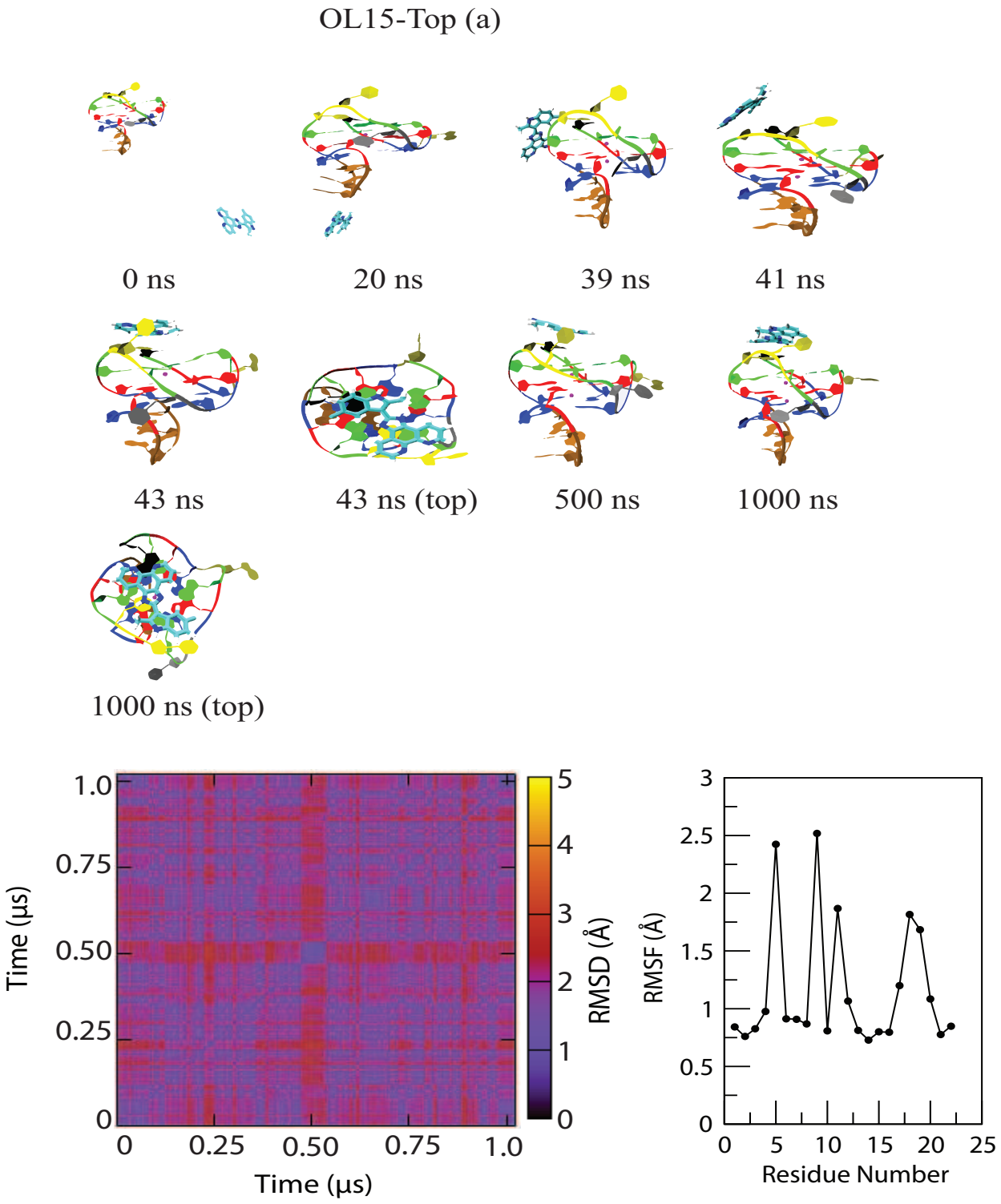

FIG. S3: (a) Snapshots representations of the complex formation of the c-KIT quadruplex DNA with time progress, (b) taking into account all heavy atoms of c-KIT G-quadruplex DNA, pairwise 2D-RMSDs of different systems, and (c) Root-mean-square fluctuations (RMSFs) of all heavy atom of c-KIT G-quadruplex DNA for different systems.

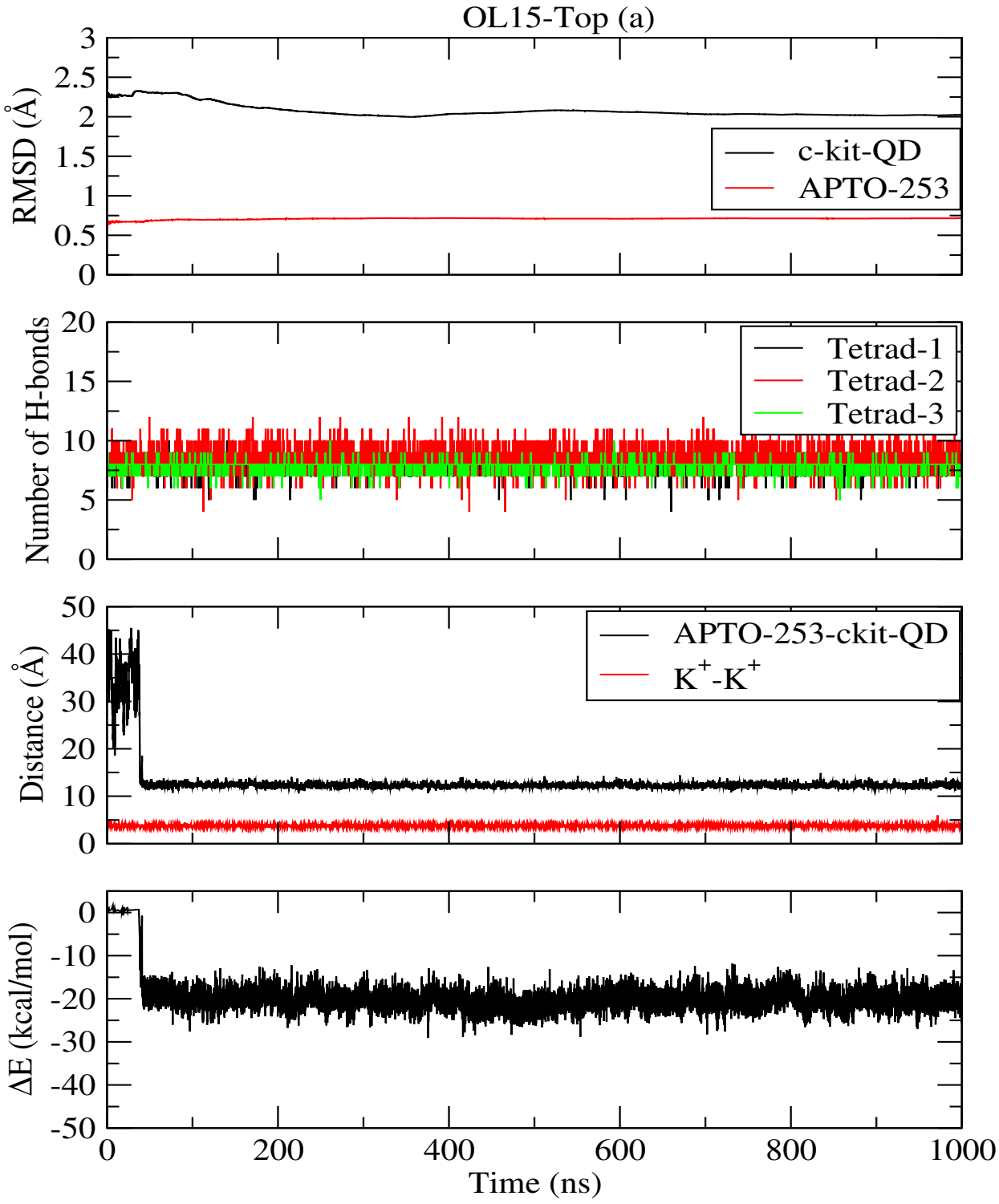

FIG. S4: (a) Time progression of the root-mean-square deviations (RMSDs) of all heavy atom of c-KIT G-quadruplex DNA, (b) number of hydrogen bonds for tetrads, (c) the distance between center of masses of c-KIT G-quadruplex DNA and APTO-253, and the distance between the two K^+ central cations, and (d) the binding free energy of complex formation of APTO-253 ligand and c-KIT G-quadruplex DNA with time progression.

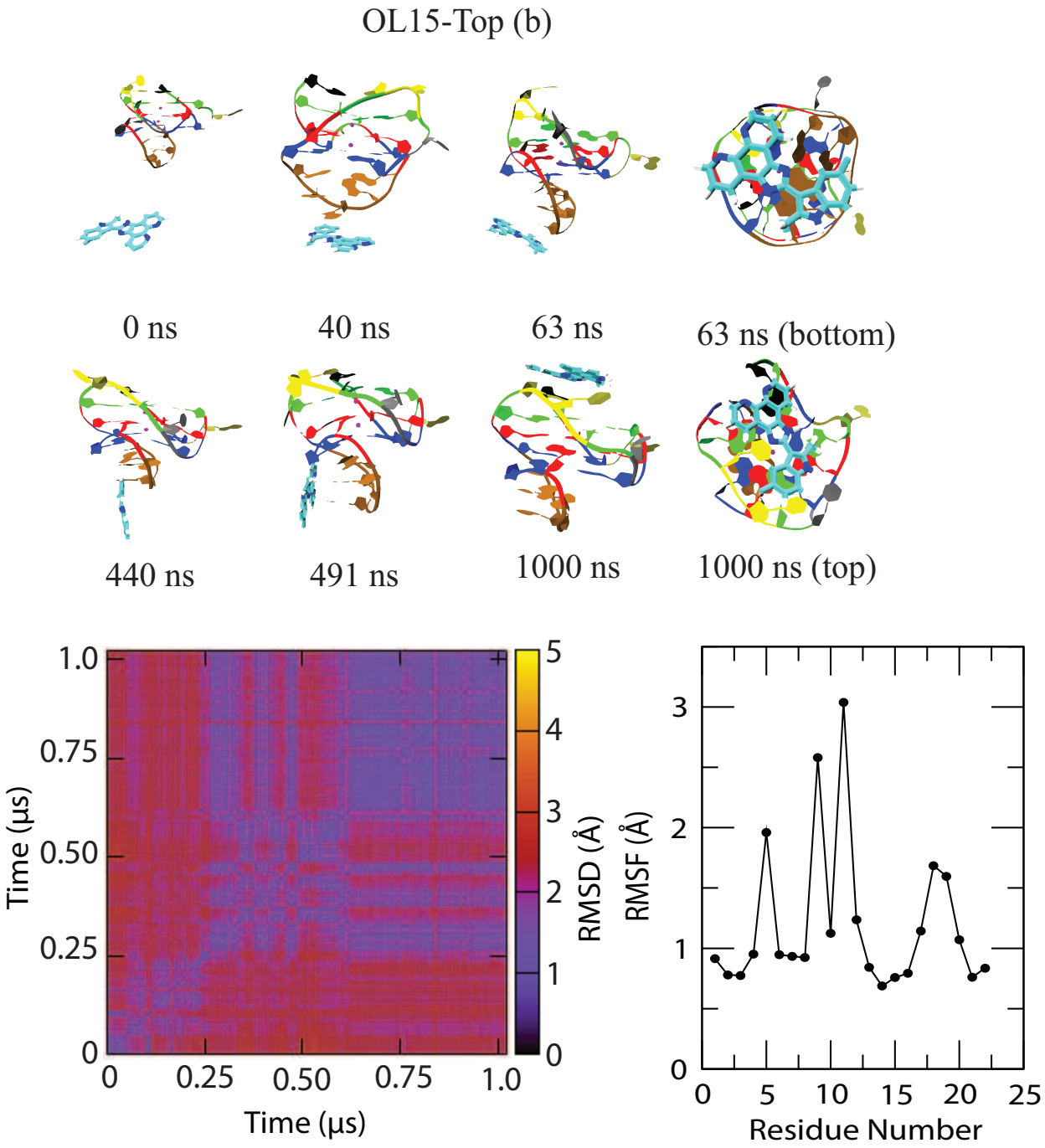

FIG. S5: (a) Snapshots representations of the complex formation of the c-KIT quadruplex DNA with time progress, (b) taking into account all heavy atoms of c-KIT G-quadruplex DNA, pairwise 2D-RMSDs of different systems, and (c) Root-mean-square fluctuations (RMSFs) of all heavy atom of c-KIT G-quadruplex DNA for different systems.

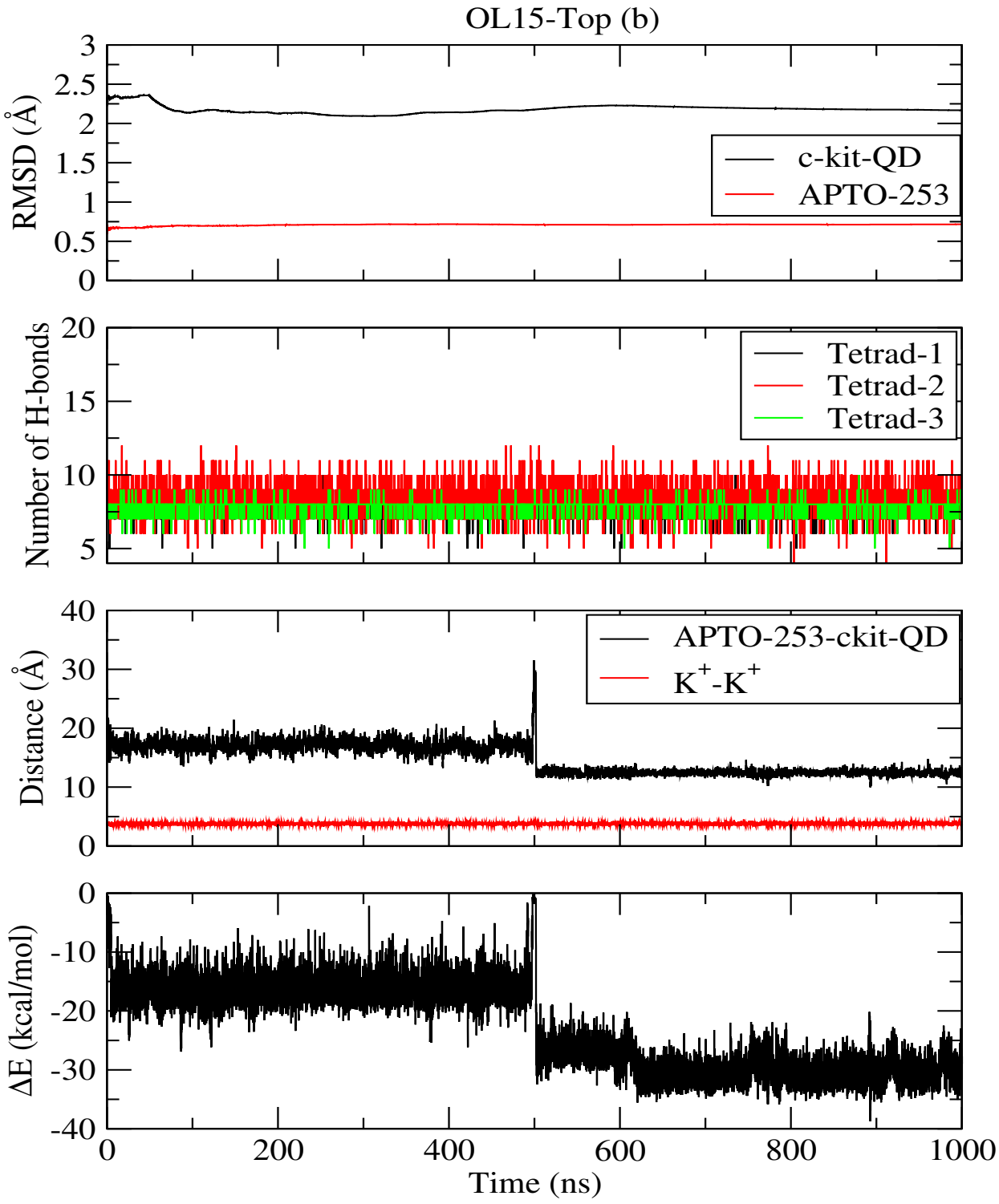

FIG. S6: (a) Time progression of the root-mean-square deviations (RMSDs) of all heavy atom of c-KIT G-quadruplex DNA, (b) number of hydrogen bonds for tetrads, (c) the distance between center of masses of c-KIT G-quadruplex DNA and APTO-253, and the distance between the two K^+ central cations, and (d) the binding free energy of complex formation of APTO-253 ligand and c-KIT G-quadruplex DNA with time progression.

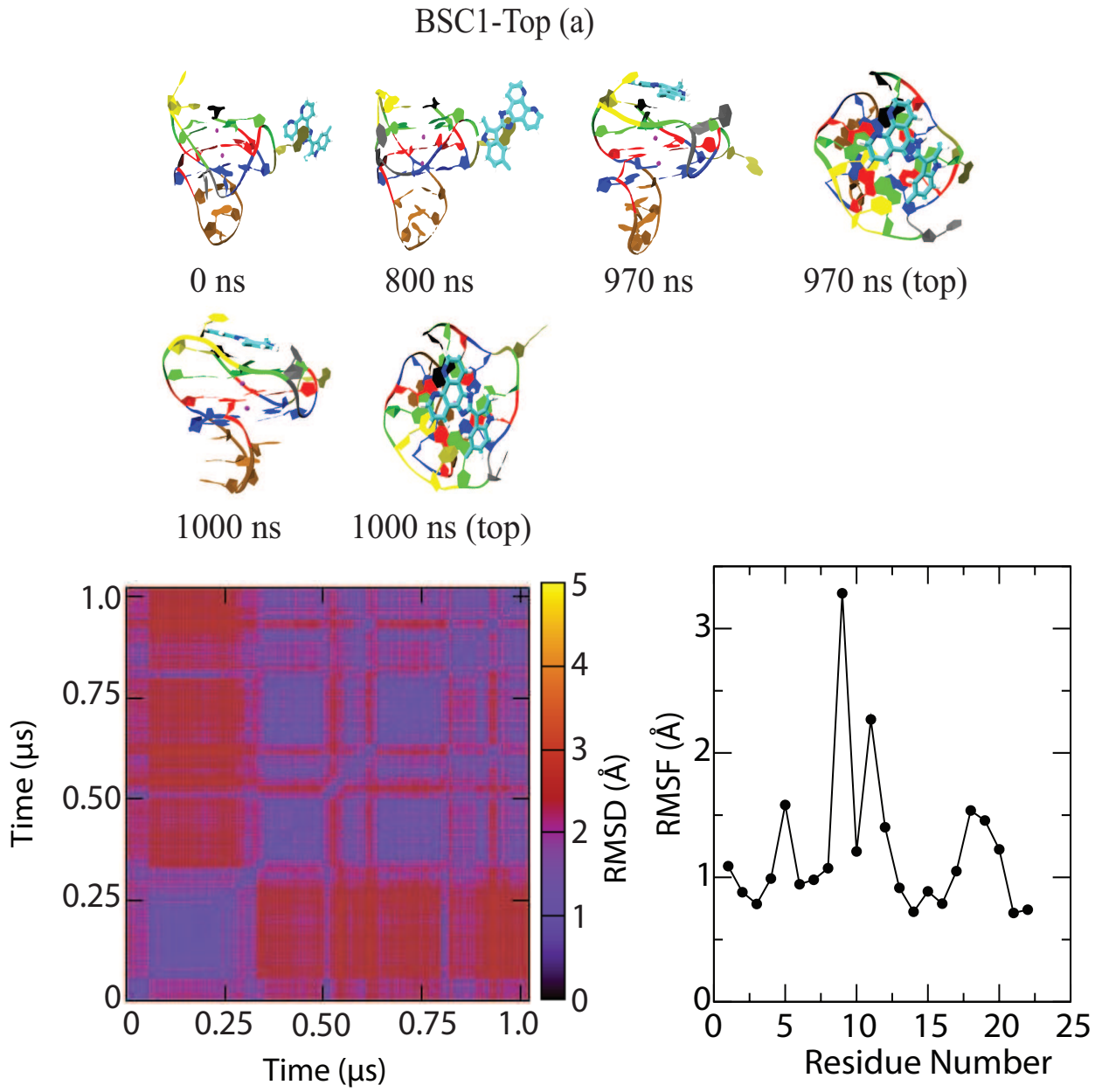

FIG. S7: (a) Snapshots representations of the complex formation of the c-KIT quadruplex DNA with time progress, (b) taking into account all heavy atoms of c-KIT G-quadruplex DNA, pairwise 2D-RMSDs of different systems, and (c) Root-mean-square fluctuations (RMSFs) of all heavy atom of c-KIT G-quadruplex DNA for different systems.

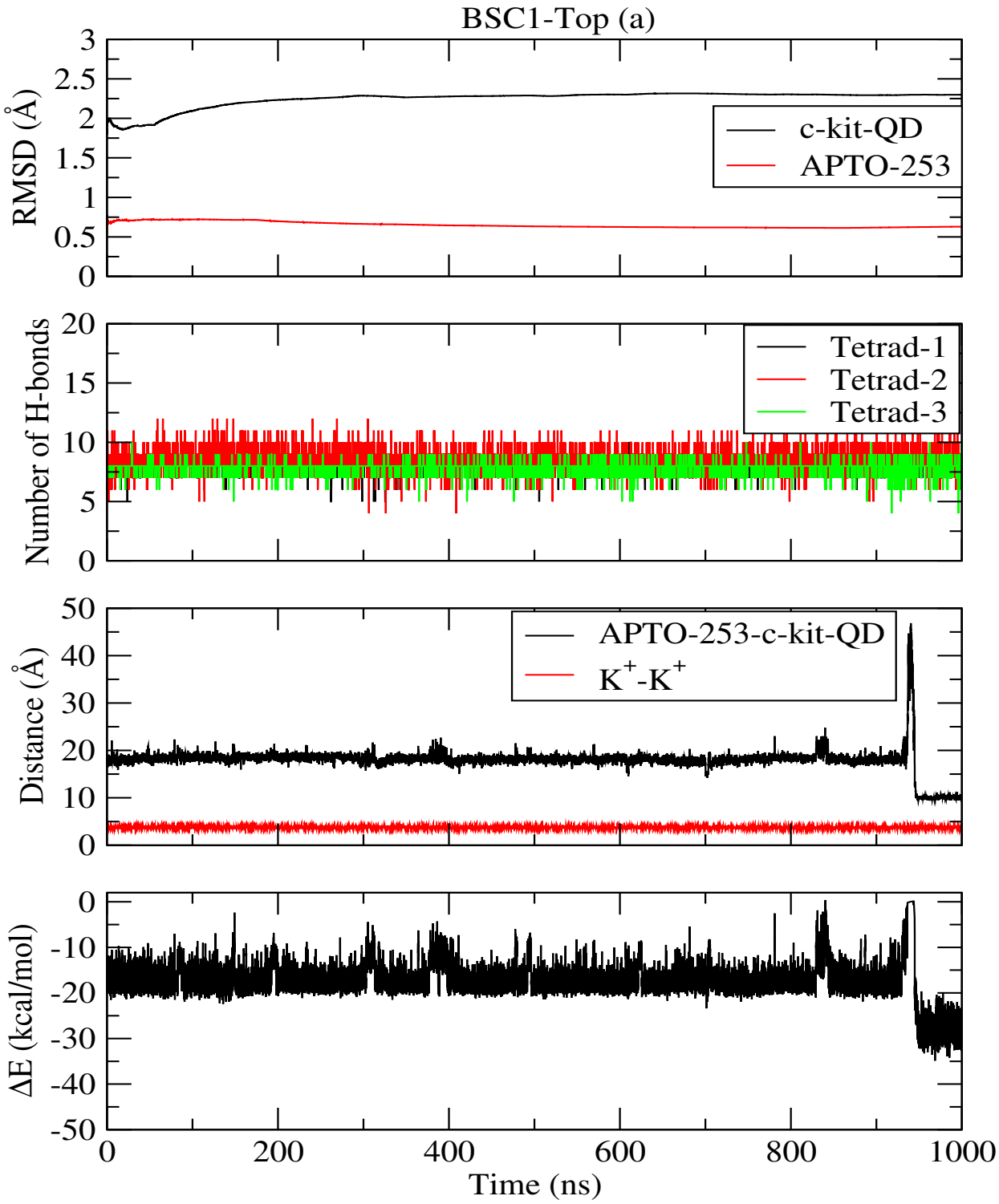

FIG. S8: (a) Time progression of the root-mean-square deviations (RMSDs) of all heavy atom of c-KIT G-quadruplex DNA, (b) number of hydrogen bonds for tetrads, (c) the distance between center of masses of c-KIT G-quadruplex DNA and APTO-253, and the distance between the two K^+ central cations, and (d) the binding free energy of complex formation of APTO-253 ligand and c-KIT G-quadruplex DNA with time progression.

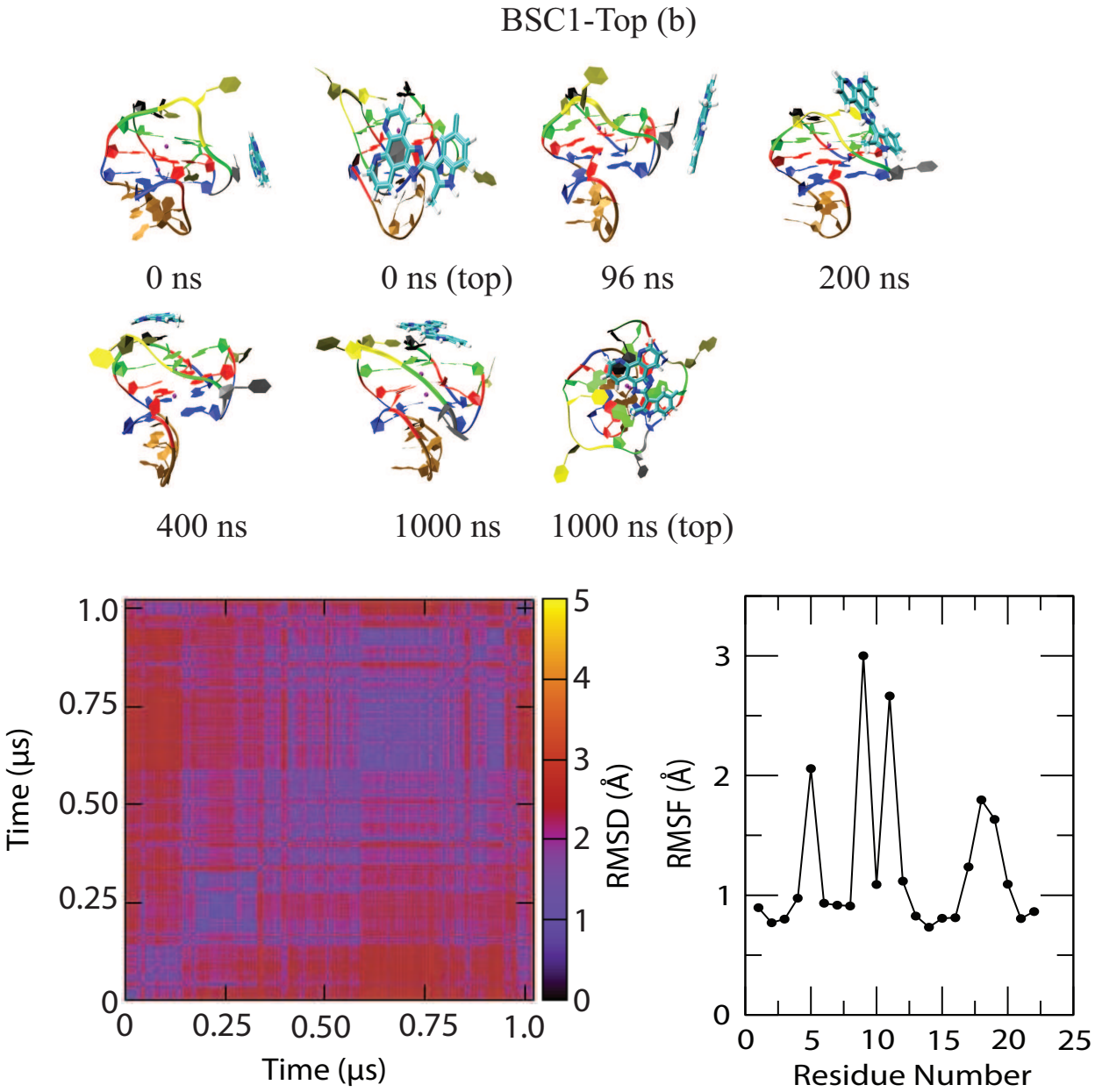

FIG. S9: (a) Snapshots representations of the complex formation of the c-KIT quadruplex DNA with time progress, (b) taking into account all heavy atoms of c-KIT G-quadruplex DNA, pairwise 2D-RMSDs of different systems, and (c) Root-mean-square fluctuations (RMSFs) of all heavy atom of c-KIT G-quadruplex DNA for different systems.

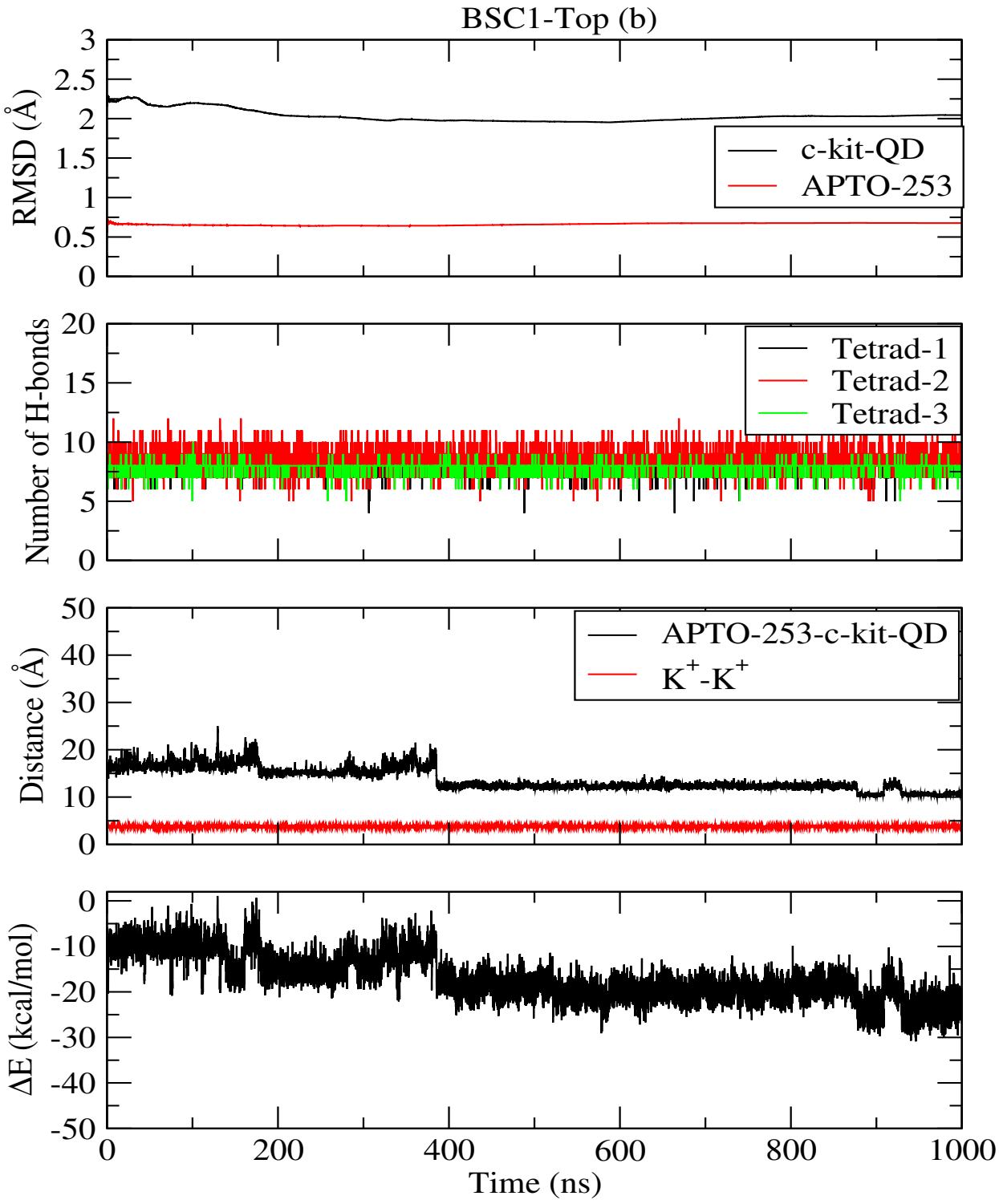

FIG. S10: (a) Time progression of the root-mean-square deviations (RMSDs) of all heavy atom of c-KIT G-quadruplex DNA, (b) number of hydrogen bonds for tetrads, (c) the distance between center of masses of c-KIT G-quadruplex DNA and APTO-253, and the distance between the two K^+ central cations, and (d) the binding free energy of complex formation of APTO-253 ligand and c-KIT G-quadruplex DNA with time progression.

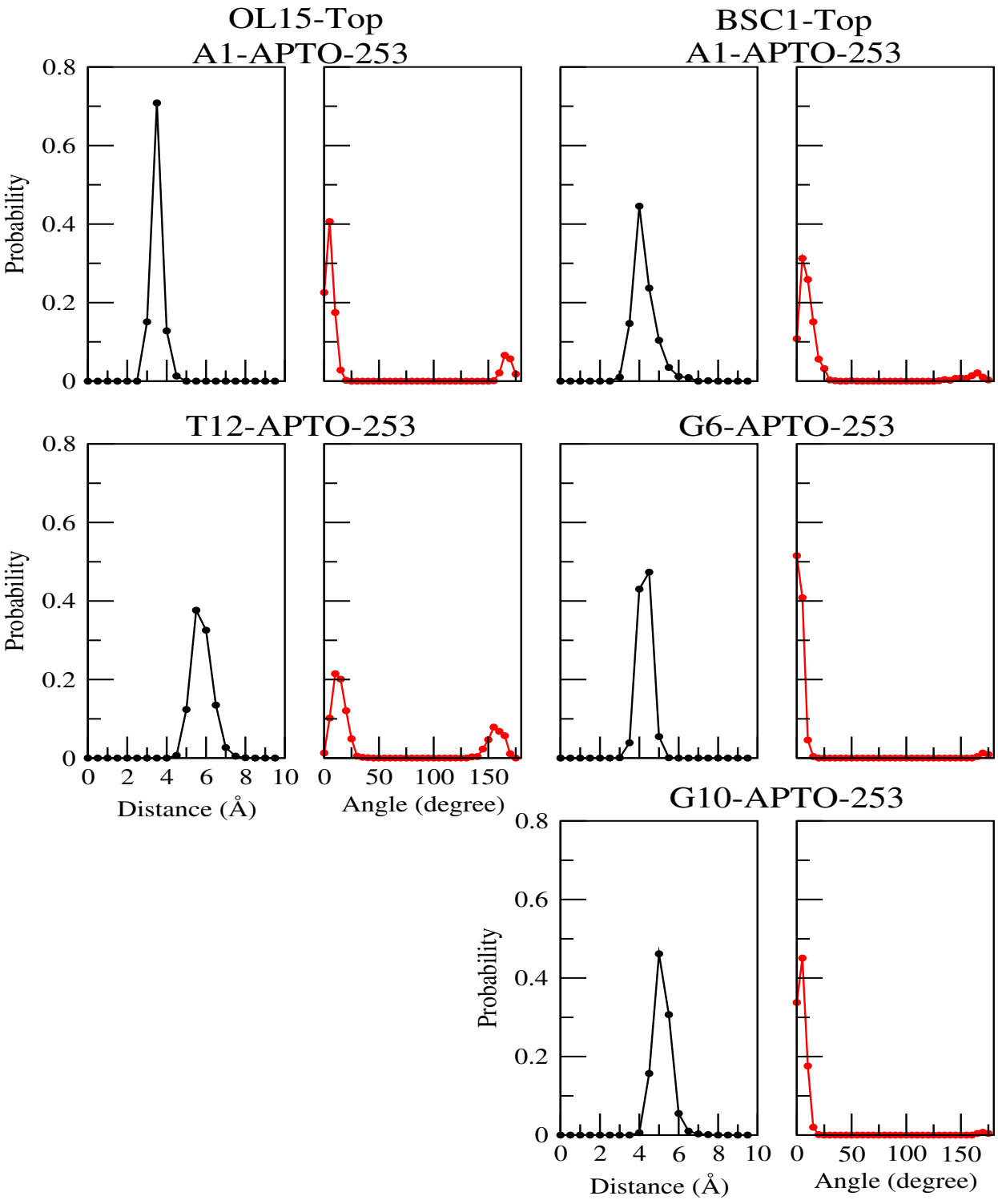

FIG. S11: Stacking probability with respect to distance and angle between the corresponding planes.

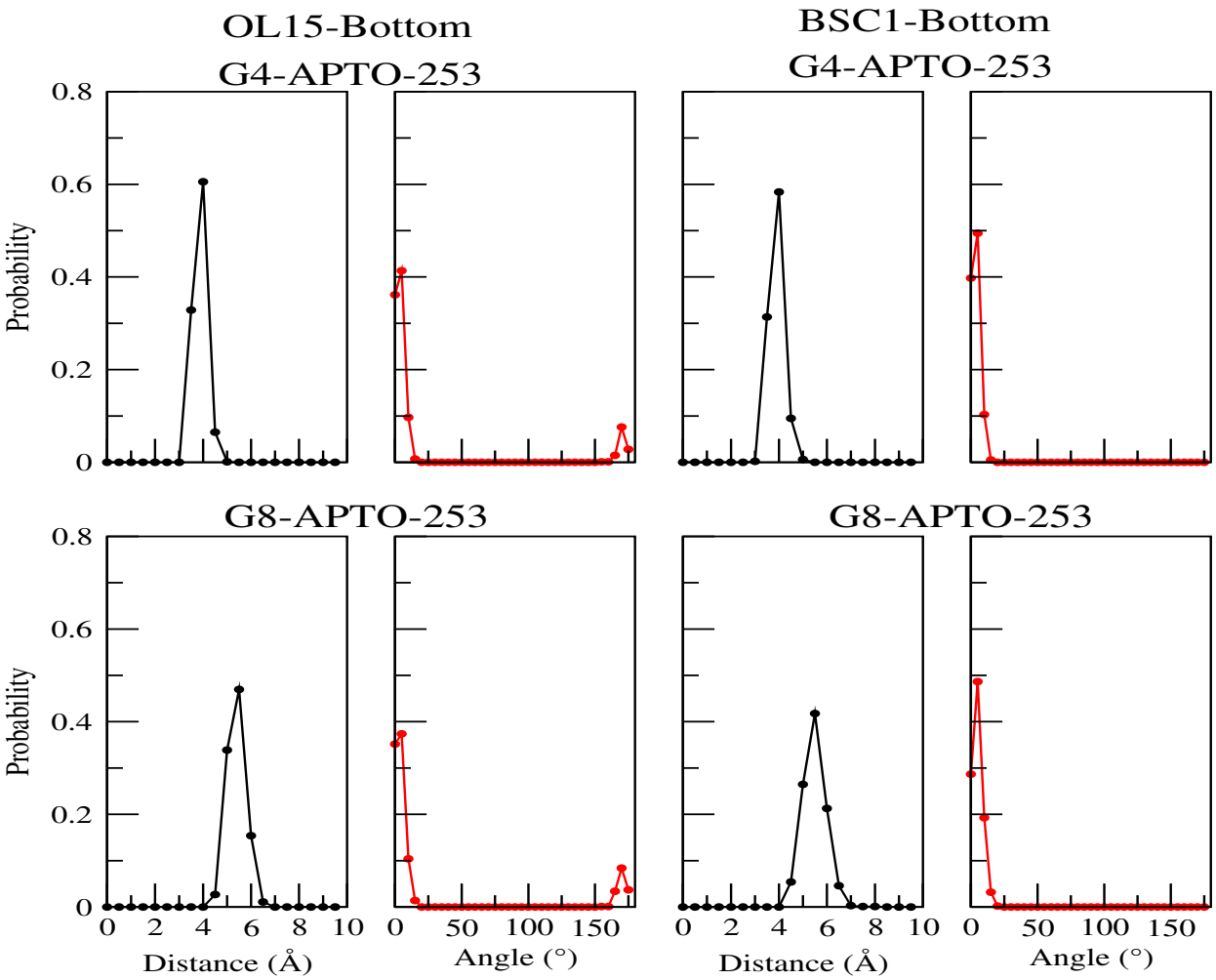

FIG. S12: Stacking probability with respect to distance and angle between the corresponding planes.

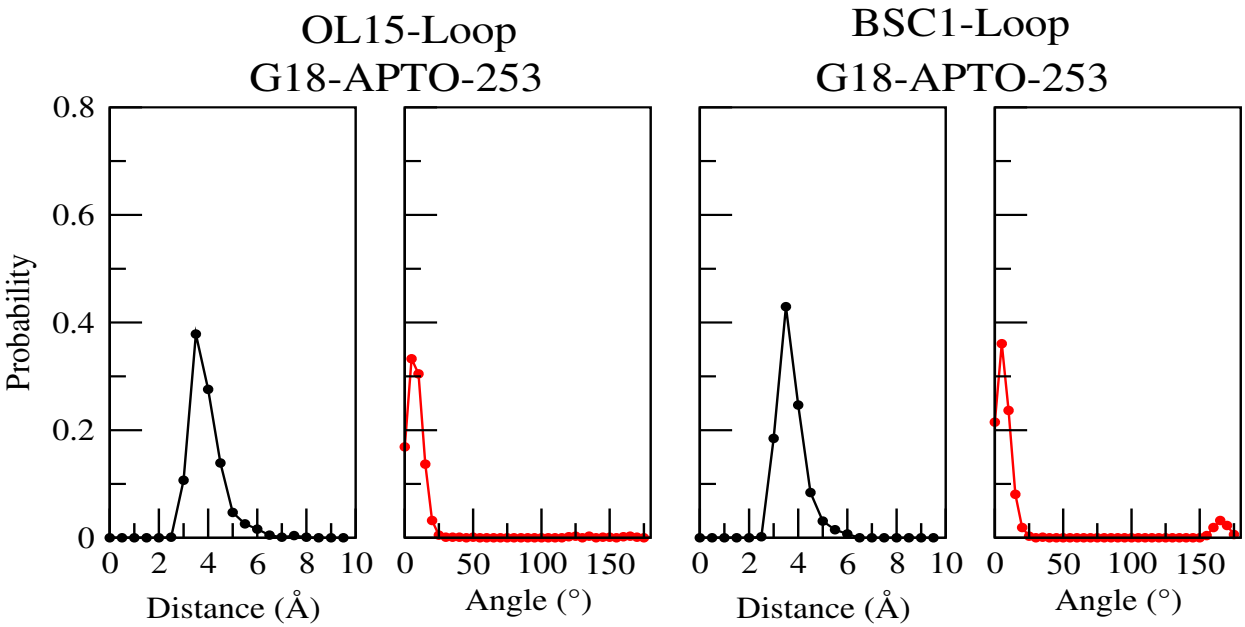

FIG. S13: Stacking probability with respect to distance and angle between the corresponding planes.

* Electronic address: sandipp@iitg.ac.in